Int J Adv Manuf Technol (2015) 77:1599–1611
DOI 10.1007/s00170-014-6366-6

ORIGINAL ARTICLE

# Comparison of injection molding process windows for plastic lens established by artificial neural network and response surface methodology

**Kuo-Ming Tsai · Hao-Jhih Luo**

Received: 17 March 2014 / Accepted: 8 September 2014 / Published online: 14 November 2014


**Abstract** This study used artificial neural network (ANN) and response surface methodology (RSM) to obtain the lens form accuracy prediction model. Moreover, it established the operating parameter region that satisfies the designated lens form accuracy at a minimum cost. Finally, experimental verification and accuracy comparison were conducted. This study used the Taguchi method for parameter screening experiment in the injection molding process. The obtained significant factors that influence form accuracy of the lens were mold temperature, cooling time, and packing time. Those significant factors were used for full factorial experiment, for adjusted experiment using composite central design method, and to establish the process window. According to the results, the process window for injection molding using an ANN to establish cooling time and packing time was a high-order, irregular shape, whereas the one established by a RSM was oblique oval. The optimal form accuracy of the lens obtained from ANN model was better than that from RSM model. The result of the experiment indicated that the process window of the injection molding process for optimal form accuracy obtained from both ANN and RSM models is quite consistent. In addition, a case study for a form accuracy of 0.5 μm was discussed. The process window established by ANN had a better accuracy and wider range than that by RSM.

**Keywords** Process window · Injection molding · Optical lens · Artificial neural network (ANN) · Response surface methodology (RSM)

K.-M. Tsai (✉) · H.-J. Luo
Department of Mechanical Engineering, National Chin-Yi University of Technology, Taichung, Taiwan, Republic of China
e-mail: tsai101@ncut.edu.tw

## 1 Introduction

Plastic injection molding process is characterized by high efficiency, high yield, low cost, easy automation, and applicability to complex products. It has been used as the crucial technique for producing plastic lens. Injection molding process is divided into several stages according to the operating cycles, including plasticization, filling, packing, cooling, and ejection. First, the plastic pellets are plasticized into melt after screw shearing and feed pipe heating. Then, the melt is injected into the runner system of the mold to fill the cavities. Finally, the finished product is ejected after cooling. In the injection molding process, many factors influence the quality of final molded parts; thus, the quality of molded parts is highly unpredictable. The properties of plastic material, design of mold, and process parameters have significant impacts [1–3].

Traditionally, the operating conditions of injection molding often rely on workers' experience, and operating conditions for mass production are obtained through repeated mold testing. However, the mold testing process requires rich engineering experience, which is complex and time-consuming. Plastic injection molding has many related process parameters. In order to save experimental cost and time, the fractional factorial design of experiment [4–6] is usually used for screening experiments. The parameter design of the Taguchi method is an especially high-efficiency parameter screening method [7–9], and it has been widely applied to the research of injection molding [3, 10–15]. Many studies have used artificial intelligence technology to build models for relationship between process parameters and the quality of molded parts [16–20]. Different optimization methods have been applied to obtain a combination of optimal parameters for the injection molding processes [21–25]. In addition, response surface methodology (RSM) is a model-building research method that

incorporates statistics [26–28]. The method is usually used to determine the optimum operating parameters of a system [29–34].

Previous studies have reported that the quality of injection molded parts depends on product shape, mold design, plastic properties, and molding conditions. Multiple operating conditions have been used to determine parameter combinations of the best quality for building process models. By reverse modeling, this study determines the appropriate operating parameter range according to the quality specification of products required and obtains a process window that conforms to the quality at a minimum cost. Therefore, this study uses the form accuracy of the spherical lens, or quality characteristic, known as peak-to-valley (PV) value, as well as the Taguchi method, to screen the combination of optimal process factors and its significant factors. The artificial neural network (ANN) and RSM models are obtained by a full factorial experiment of significant factors. Finally, two process windows are established by curve fitting and their results are compared for accuracy.

## 2 Fundamental theory

### 2.1 Response surface methodology

This study used the significant factors obtained from the Taguchi experiment to establish RSM model for form accuracy of the lens which was the following quadratic polynomial equation with interaction:

$$\begin{aligned} y &= \beta_0 + \sum_i \beta_i x_i + \sum_i \beta_{ii} x_i^2 + \sum_{i<j} \beta_{ij} x_i x_j + \sum_{i,j} \beta_{ij} x_i x_j^2 + \varepsilon \\ &= \beta_0 + \beta_1 A + \beta_2 \beta + \beta_3 C + \beta_4 AB + \beta_5 AC + \beta_6 BC \\ &\quad + \beta_7 ABC + \beta_8 A^2 + \beta_9 B^2 \\ &= +\beta_{10} C^2 + \beta_{11} A^2 B + \beta_{12} A^2 C + \beta_{13} AB^2 + \beta_{14} AC^2 \\ &\quad + \beta_{15} B^2 C + \beta_{16} BC^2 + \varepsilon \end{aligned} \tag{1}$$

where $y$ is the response variable; $\beta$ is the undetermined coefficient; $x$, $A$, $B$, and $C$ are independent variables; and $\varepsilon$ is the model error.

### 2.2 Artificial neural network

The artificial neural network is a parallel computational model that is similar to the animal neuromechanism, namely, using computer calculation to simulate human cerebral nerve cell network. The difficulty of building a traditional mathematical model is that assumptions or simplification conditions are needed when solving complex and highly nonlinear problems. However, the simplified model may be different from the actual phenomenon. ANN does not define complex mathematical models according to problems but handles complex and probabilistic problems by learning and memorizing. Therefore, it has a good effect on handling classification, function approximation, optimization, and prediction problems [21].

#### 2.2.1 Back-propagation neural network

The back-propagation neural network (BPNN) is one of the most representative and popular neural networks among numerous neural networks. BPNN is a multilayer, feedforward network and uses a supervised learning method to handle the nonlinear relations between input and output variables. This study uses a BPNN to build an optical lens form accuracy prediction model. The activation function for the hidden layer and output layer of the network is a positive logarithmic sigmoid function, and the input-output relationship is

$$f(\text{net}) = \frac{1}{1 + e^{-(\lambda \text{net})}} \tag{2}$$

where net is the aggregation function of neurons and $\lambda$ is the gain factor of neurons. The values of this activation function approaches 0 and 1, respectively, when the independent variable approaches a plus-minus infinity, as shown in Fig. 1.

#### 2.2.2 Network performance function definition

In the process of training ANN of this study, the performance function is represented by mean square error (MSE), i.e., the

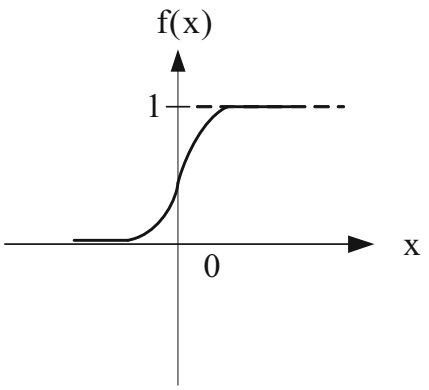


**Fig. 1** Positive logistic function

average of square errors between neural network inference value and target value, defined as follows:

$$\mathrm{MSE} = \frac{1}{n}\sum_{i=1}^{n}(T_i - A_i)^2 \tag{3}$$

where $T_i$ is the target value of no. $i$ group, $A_i$ is the network inference value of no. $i$ group, and $n$ is the number of training samples.

### 2.3 Coefficient of determination

In the ANN and RSM models, in order to express the fitness of the model for experimental data, the coefficient of determination ($R^2$) is often used to determine the accuracy of the model. The larger the $R^2$ is, the better the fitness will be, i.e., the closer the model predicted value will be to the experimental value. $R^2$ is defined [5] as

$$R^2 = \frac{\text{Regression sum of squares (SSR)}}{\text{Total sum of squares (SST)}} = 1 - \frac{\text{Error sum of squares (SSE)}}{\text{Total sum of squares (SST)}} \tag{4}$$

where total sum of squares (SST) is the total variance, regression sum of squares (SSR) is the amount of variation that can be explained by the model, and error sum of squares (SSE) is the amount of random variation that cannot yet be explained by the model.

## 3 Experiment setup

This study experimentally establishes the injection molding process windows for optical lenses, and confirmation experiments are then performed to verify the validity of the windows. The overall research procedure is shown in Fig. 2.

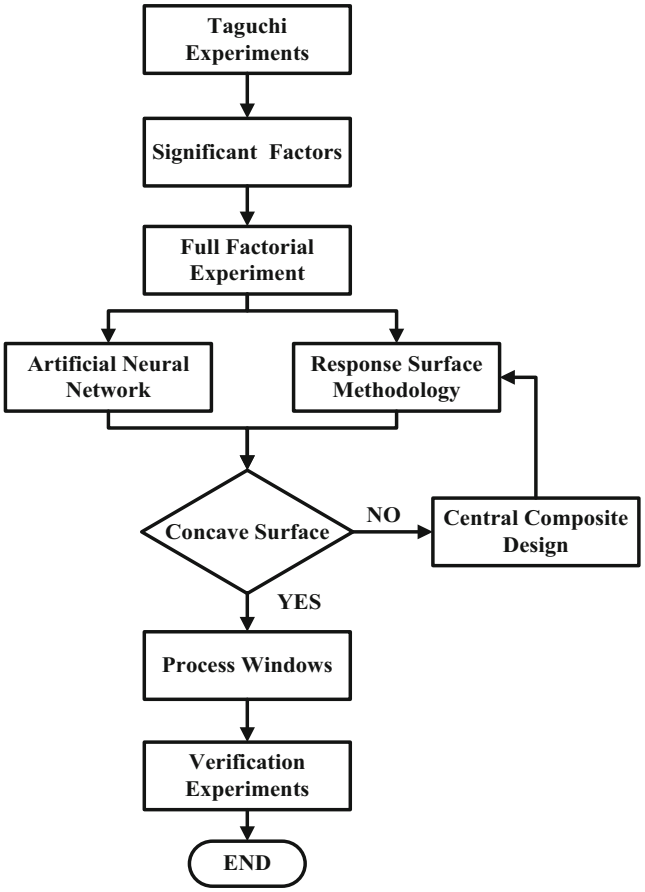


**Fig. 2** Flow chart for this study

### 3.1 Lens specifications

The diameter of the lens is 6 mm, the effective spherical diameter of the lens is 5 mm, and the maximum thickness at the lens center is 0.66 mm. A plano-convex lens is adopted, as shown in Fig. 3a, and a four-cavity layout of product is designed in a mold, as shown in Fig. 3b.

### 3.2 Experimental equipment and material

Injection molding machine and measuring instruments are used in this study. A 220S 250-60 precision injection molding machine produced by Arburg (Germany) was used for injection molding experiments. The surface form accuracy of the lens was measured by the Form Talysurf PGI-840 made by Taylor Hobson (Britain). The experimental material was optical-grade polymethyl methacrylate (PMMA)-80N, manufactured by Asahi Kasei (Japan). Five specimens were sampled at the same cavity of the four-cavity mold and the average value was taken as the experimental data. The curve fitting, response surface modeling, ANN modeling, and their plotting programs for experimental data were generated using MATLAB® with neural network Toolbox (R2012a).

## 4 Results and discussion

### 4.1 Form accuracy model for RSM

This study investigates the form accuracy of spherical lens through the Taguchi experiment; it is a smaller-the-better

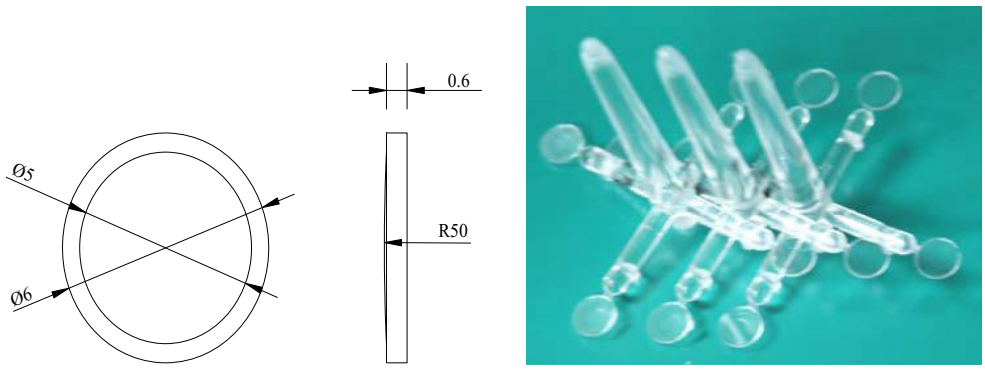


(a) Dimensions of lens. (b) Molded Product.

**Fig. 3** Dimensions of the plano-convex lens (**a**) and a photograph of the molded product (**b**)

(STB) quality characteristic. The eight control factors are selected as shown in Table 1, i.e., melt temperature, injection speed, injection pressure, packing pressure, packing time, filling-to-packing switchover position, mold temperature, and cooling time. A $L_{18}(2^1 \times 3^7)$ orthogonal array was used and then the experimental result is shown in Table 2. Analysis of variance (ANOVA) is used to implement and identify the influence of control factors for the Taguchi experiment. Table 3 is the ANOVA table for STB signal/noise (S/N) ratio of the lens form accuracy, in which the most significant influence is the mold temperature. The result observed that the optimal parameter levels combination is $A_2B_1C_1D_1E_2F_1$-$G_2H_3$, i.e., melt temperature of 250 °C, injection speed of 30 mm/s, injection pressure of 100 MPa, packing pressure of 10 MPa, packing time of 2 s, filling-to-packing switchover position of 4.64 mm, mold temperature of 80 °C, and cooling time of 12 s. And the Taguchi experiment result is reliable via the confirmation experiments. In addition, according to contribution rate, three control factors are selected for $3^3$ full factorial experiments to obtain data points for constructing process window: mold temperature, cooling time, and packing time. In order to obtain better lens form accuracy, the range of mold temperature is reset to 70 °C to 100 °C because the form accuracy of the lens is worse at a mold temperature of 60 °C for the Taguchi experiment. The cooling time and packing time are maintained within the range of the Taguchi experiment, while the remaining process parameters use the optimal factor level combination derived from the Taguchi experiment. The adjusted limits of the three significant parameters for $3^3$ full factorial experiments are shown in Table 4, and the response surface with contour diagrams at a mold temperature of 70 °C is shown in Fig. 4.

**Table 1** Factors and levels for the Taguchi experiment

| Control factor | Level 1 | Level 2 | Level 3 |
|---|---|---|---|
| Melt temperature (°C) | 230 | 250 | |
| Injection speed (mm/s) | 30 | 40 | 50 |
| Injection pressure (MPa) | 100 | 110 | 120 |
| Packing pressure (MPa) | 10 | 20 | 30 |
| Packing time (s) | 1 | 2 | 3 |
| Switchover position (mm) | 4.64 | 4.74 | 4.84 |
| Mold temperature (°C) | 60 | 80 | 100 |
| Cooling time (s) | 8 | 10 | 12 |

In order to obtain the process windows for the best quality, RSM models need to be concave surfaces. According to Fig. 4, the response surface was not a concave surface, suggesting that the cooling time and packing time chosen in this experiment were not appropriate. Therefore, a composite central design (CCD) in the direction of steepest descent was used to adjust the level of parameters and redo the experiments until a concave surface is obtained and optimal form accuracy is achieved. Based on the steepest descent of lens form accuracy at a mold temperature of 70 °C, the range of experimental parameters is translated and the new limits of the parameters are cooling times of 10 and 14 s and packing times of 1 and 2 s. Therefore, the center point of CCD is a cooling time of 10 s and a packing time of 1.5 s. In addition, the factor value of $\alpha$ of the axial point for the two-factor CCD is $\sqrt{2}$, e.g., the actual experimental values are cooling times of 9.2 and 14.8 s and packing times of 0.8 and 2.2 s, where $\alpha$ is the distance from the CCD center. The adjusted levels for the two significant parameters are shown in Table 5, and the response surface contour diagram at mold temperature of 70 °C is shown in Fig. 5. The concave surface model at a mold temperature of 70 °C has been obtained. Consequently, the factor levels of experimental parameters for fitting response surface model can be adjusted, and the limits for the three significant parameters are shown in Table 6. RSM models for the form accuracy of lenses based on three injection molding parameters can be identified using the experimental data of the concave surfaces. The fitting and verifying procedure of RSM model for form accuracy of the lens that has been

**Table 2** Form accuracies and S/N ratio for $L_{18}(2^1\times3^7)$

| Run | Control factor | | | | | | | | PV (μm) | $\sigma$ (μm) | S/N (dB) |
|---|---|---|---|---|---|---|---|---|---|---|---|
| | *A* | *B* | *C* | *D* | *E* | *F* | *G* | *H* | | | |
| 1 | 1 | 1 | 1 | 1 | 1 | 1 | 1 | 1 | 1.3181 | 0.2351 | −2.3987 |
| 2 | 1 | 1 | 2 | 2 | 2 | 2 | 2 | 2 | 0.5981 | 0.0988 | 4.4645 |
| 3 | 1 | 1 | 3 | 3 | 3 | 3 | 3 | 3 | 0.5742 | 0.1000 | 4.8187 |
| 4 | 1 | 2 | 1 | 1 | 2 | 2 | 3 | 3 | 0.3837 | 0.0529 | 8.3202 |
| 5 | 1 | 2 | 2 | 2 | 3 | 3 | 1 | 1 | 2.3017 | 0.2502 | −7.2410 |
| 6 | 1 | 2 | 3 | 3 | 1 | 1 | 2 | 2 | 0.4485 | 0.1013 | 6.9644 |
| 7 | 1 | 3 | 1 | 2 | 1 | 3 | 2 | 3 | 0.4287 | 0.0837 | 7.3573 |
| 8 | 1 | 3 | 2 | 3 | 2 | 1 | 3 | 1 | 0.4622 | 0.1004 | 6.7038 |
| 9 | 1 | 3 | 3 | 1 | 3 | 2 | 1 | 2 | 1.7348 | 0.2015 | −4.7848 |
| 10 | 2 | 1 | 1 | 3 | 3 | 2 | 2 | 1 | 0.5839 | 0.1131 | 4.6729 |
| 11 | 2 | 1 | 2 | 1 | 1 | 3 | 3 | 2 | 0.5159 | 0.1014 | 5.7480 |
| 12 | 2 | 1 | 3 | 2 | 2 | 1 | 1 | 3 | 0.6822 | 0.0824 | 3.3220 |
| 13 | 2 | 2 | 1 | 2 | 3 | 1 | 3 | 2 | 0.5230 | 0.1024 | 5.6303 |
| 14 | 2 | 2 | 2 | 3 | 1 | 2 | 1 | 3 | 1.0510 | 0.1041 | −0.4322 |
| 15 | 2 | 2 | 3 | 1 | 2 | 3 | 2 | 1 | 0.4460 | 0.0902 | 7.0129 |
| 16 | 2 | 3 | 1 | 3 | 2 | 3 | 1 | 2 | 1.1504 | 0.1167 | −1.2173 |
| 17 | 2 | 3 | 2 | 1 | 3 | 1 | 2 | 3 | 0.3715 | 0.0374 | 8.6018 |
| 18 | 2 | 3 | 3 | 2 | 1 | 2 | 3 | 1 | 0.6771 | 0.0786 | 3.3864 |

proposed by the authors in a former paper was the following quadratic polynomial equation with interaction [35]:

$$\begin{aligned} PV = {} & 35.0636 - 0.6493M_T - 4.3466T_C + 3.1836T_P \\ & + 0.0735M_T{\cdot}T_C - 0.0792M_T{\cdot}T_P + 0.0692T_C{\cdot}T_P \\ & - 0.0002M_T{\cdot}T_C{\cdot}T_P + 0.0034{M_T}^2 + 0.0719{T_C}^2 \\ & - 0.05083{T_P}^2 - 0.0004{M_T}^2{\cdot}T_C + 0.0003{M_T}^2{\cdot}T_P \\ & - 0.0005M_T{\cdot}{T_C}^2 + 0.0085M_T{\cdot}{T_P}^2 - 0.0014{T_C}^2{\cdot}T_P \\ & - 0.0013T_C{\cdot}{T_P}^2 \end{aligned} \quad (5)$$

**Table 3** Analysis of variance for S/N ratio

| Factor | SS | DF | MS | *F* value | Contr. rate (%) |
|---|---|---|---|---|---|
| A | 8.7090 | 1 | 8.7090 | 7.2648 | 2.3620 |
| B | 0.0288 | 2 | 0.0144 | 0.0120 | 0.0078 |
| C | 1.7444 | 2 | 0.8722 | 0.7276 | 0.4731 |
| D | 2.9548 | 2 | 1.4774 | 1.2324 | 0.8014 |
| E | 23.8487 | 2 | 11.9243 | 9.9471 | 6.4682 |
| F | 18.1814 | 2 | 9.0907 | 7.5833 | 4.9311 |
| G | 274.9316 | 2 | 137.4658 | 114.6713 | 74.5665 |
| H | 35.9105 | 2 | 17.9553 | 14.9779 | 9.7396 |
| Residual | 2.3976 | 2 | 1.1988 | | 0.6503 |
| (Residual) | (93.7752) | (15) | (6.2517) | | |
| Total | 368.7068 | 17 | | | 100 |

$F_{(0.05,1,2)}$=18.51, $F_{(0.05,2,2)}$=19

where PV is the form accuracy of the lens, $M_T$ is the mold temperature, $T_C$ is the cooling time, and $T_P$ is the packing time. The response surface models, i.e., Eq. (5), for the form accuracy of lenses based on three injection molding parameters can be determined using the experimental data of all the concave surfaces, as shown in Table 7. It is observed that the model has a $R^2$ value of 0.8583, the averaged error is 11.13 %, and the MSE is 14.18. The result shows that this model has a well fitness. The response surface contour diagrams for cooling time and packing time at three mold temperatures based on RSM model can be plotted as shown in Fig. 6a, c, e. It is observed that the response surfaces are correctly concave surfaces.

**Table 4** Factors and levels for $3^3$ full factorial experiments

| Factors | Level 1 | Level 2 | Level 3 |
|---|---|---|---|
| Mold temperature (°C) | 70 | 85 | 100 |
| Cooling time (s) | 8 | 10 | 12 |
| Packing time (s) | 1 | 2 | 3 |
| Melt temperature (°C) | 250 | | |
| Injection speed (mm/s) | 30 | | |
| Injection pressure (MPa) | 100 | | |
| Packing pressure (MPa) | 10 | | |
| Switchover position (mm) | 4.64 | | |

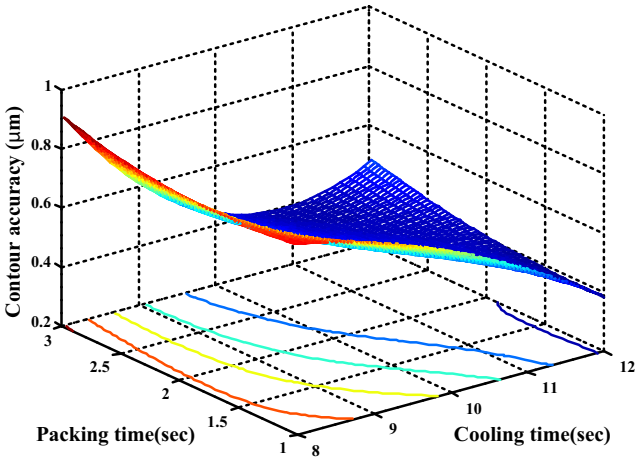


**Fig. 4** Response surfaces for the form accuracy of the lens at a mold temperature of 70 °C

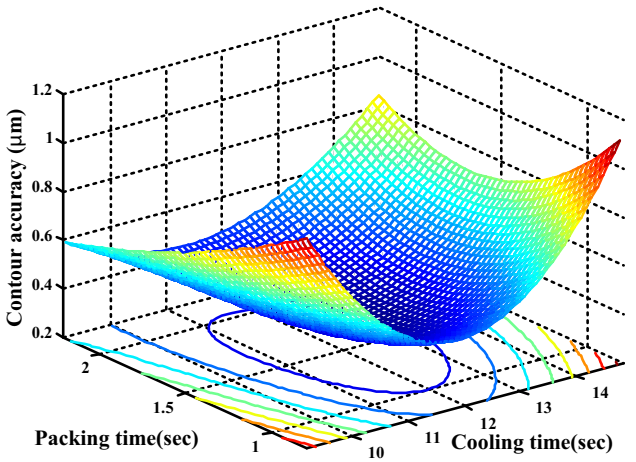


**Fig. 5** Response surface for form accuracy of the lens at a mold temperature of 70 °C after CCD experiments

## 4.2 Form accuracy model for ANN method

The supervised BPNN model is constructed according to the 34 groups of experimental data in Table 7. In that model, 22 groups are used as training samples for learning ANN model and the remaining 12 groups are used as testing samples, in order to determine the convergence step size, orientation, and stopping point of ANN. This ANN model is trained by the Levenberg-Marquardt algorithm, which has a higher network convergence rate. The other network training-related setting is a maximum training epoch of 2000, a performance goal of 0, a learning rate of 0.01, and a gradient descent at learning stop of 1E-20.

The input variable of a BPNN is the significant factor influencing the lens form accuracy. The output variable is the lens form accuracy discussed in this study, and the network architecture is as shown in Fig. 7. The number of neurons in the hidden layer is usually determined by experience or trial and error. In this study, an ANN model of 6 to 14, at intervals of two neurons, is used to compare the coefficient of determination ($R^2$) for the hidden layer. The 12 groups of testing data within Table 7 were used to implement training ANN model with different number of neurons on the hidden layer. The results are shown in Table 8. It is observed that 10 neurons model have a maximum $R^2$ value of 0.8902, and the fitness for models with other numbers of neurons is worse. Therefore, 10 neurons were used in the hidden layer. The ANN model was established by using 34 groups of experimental data and the results are shown in Table 7. The ANN model consequently has a $R^2$ value of 0.9614, the averaged error is 3.53 %, and the MSE is 7.71. Compared with the RSM model, the ANN model had a better fitness with a smaller error/MSE, because higher-order logarithmic sigmoid function was used to establish the relationship between form accuracy of the lens and the process parameters. Therefore, a better fitness for the form accuracy model can be achieved with higher-order functions. These ANN models are drawn as the response surface contour diagrams for the cooling time and packing time at different mold temperatures in Fig. 6b, d, f. The response surfaces are overall concave surfaces. Since ANN model used higher-order functions, localized apexes were observed on the response surface, as shown in Fig. 6d, f. The form accuracy contour of 0.35 μm for ANN model at a mold temperature of 70 °C presents an elliptic pedal contour as shown in Fig. 6b.

**Table 5** Factors and levels for composite central design

| Factor | Levels |
|---|---|
| Mold temperature (°C) | 70 |
| Cooling time (s) | 9.2, 10, 12, 14, 14.8 |
| Packing time (s) | 0.8, 1, 1.5, 2, 2.2 |
| Melt temperature (°C) | 250 |
| Injection speed (mm/s) | 30 |
| Injection pressure (MPa) | 100 |
| Packing pressure (MPa) | 10 |
| Transfer packing position (mm) | 4.64 |

**Table 6** Factors and levels for the experiments at two fitted models

| Factors | Levels | | |
|---|---|---|---|
| Mold temperature (°C) | 70 | 85 | 100 |
| Cooling time (s) | 8, 9.2, 10, 12, 14, 14.8 | 8, 10, 12 | 8, 10, 12 |
| Packing time (s) | 0.8, 1, 1.5, 2, 2.2, 3 | 1, 2, 3 | 1, 2, 3 |
| Melt temperature (°C) | 250 | 250 | 250 |
| Injection speed (mm/s) | 30 | 30 | 30 |
| Injection pressure (MPa) | 100 | 100 | 100 |
| Packing pressure (MPa) | 10 | 10 | 10 |
| Switchover position (mm) | 4.64 | 4.64 | 4.64 |

**Table 7** Form accuracy of lenses for the experiments at two fitted models

| Run | Mold temp (°C) | Cool time (s) | Pack time (s) | Exp. PV (μm) | RSM pred. PV (μm) | RSM error (%) | ANN pred. PV (μm) | ANN error (%) | ANN data set |
|---|---|---|---|---|---|---|---|---|---|
| 1 | 70 | 8 | 1 | 0.8399 | 0.9931 | 18.24 | 0.7721 | 8.07 | c |
| 2 | 70 | 8 | 2 | 0.8343 | 0.8446 | 1.24 | 0.8343 | 0 | t |
| 3 | 70 | 8 | 3 | 0.9084 | 0.8434 | 7.15 | 0.9227 | 1.57 | c |
| 4 | 70 | 10 | 1 | 0.6885 | 0.5756 | 16.40 | 0.6885 | 0 | t |
| 5 | 70 | 10 | 2 | 0.5036 | 0.4854 | 3.62 | 0.5036 | 0 | t |
| 6 | 70 | 10 | 3 | 0.4531 | 0.5375 | 18.62 | 0.4517 | 0.31 | c |
| 7 | 70 | 12 | 1 | 0.3802 | 0.4509 | 18.60 | 0.3802 | 0 | t |
| 8 | 70 | 12 | 2 | 0.4128 | 0.4078 | 1.20 | 0.3442 | 16.62 | c |
| 9 | 70 | 12 | 3 | 0.4837 | 0.5019 | 3.77 | 0.4837 | 0 | t |
| 10 | 70 | 14 | 1 | 0.6923 | 0.6190 | 10.59 | 0.6923 | 0 | t |
| 11 | 70 | 14 | 2 | 0.6049 | 0.6118 | 1.14 | 0.5210 | 13.87 | c |
| 12 | 70 | 9.17 | 1.5 | 0.7732 | 0.6387 | 17.39 | 0.7732 | 0 | t |
| 13 | 70 | 14.83 | 1.5 | 0.7419 | 0.7606 | 2.52 | 0.7419 | 0 | t |
| 14 | 70 | 12 | 0.79 | 0.4768 | 0.4774 | 0.13 | 0.4768 | 0 | t |
| 15 | 70 | 12 | 2.21 | 0.4643 | 0.4162 | 10.36 | 0.3415 | 26.45 | c |
| 16 | 70 | 12 | 1.5 | 0.3186 | 0.4122 | 29.36 | 0.3186 | 0 | t |
| 17 | 85 | 8 | 1 | 0.7477 | 0.6512 | 12.91 | 0.5823 | 22.12 | c |
| 18 | 85 | 8 | 2 | 0.5043 | 0.4434 | 12.07 | 0.5043 | 0 | t |
| 19 | 85 | 8 | 3 | 0.5288 | 0.6368 | 20.41 | 0.5288 | 0 | t |
| 20 | 85 | 10 | 1 | 0.5471 | 0.5373 | 1.78 | 0.5471 | 0 | t |
| 21 | 85 | 10 | 2 | 0.2638 | 0.3831 | 45.25 | 0.2558 | 3.03 | c |
| 22 | 85 | 10 | 3 | 0.6357 | 0.6250 | 1.69 | 0.6357 | 0 | t |
| 23 | 85 | 12 | 1 | 0.6208 | 0.6581 | 6.02 | 0.6208 | 0 | t |
| 24 | 85 | 12 | 2 | 0.4671 | 0.5463 | 16.95 | 0.4018 | 13.98 | c |
| 25 | 85 | 12 | 3 | 0.9916 | 0.8255 | 16.75 | 0.9916 | 0 | t |
| 26 | 100 | 8 | 1 | 0.7041 | 0.7201 | 2.27 | 0.6519 | 7.41 | c |
| 27 | 100 | 8 | 2 | 0.5458 | 0.6016 | 10.22 | 0.5458 | 0 | t |
| 28 | 100 | 8 | 3 | 1.1852 | 1.1380 | 3.98 | 1.1852 | 0 | t |
| 29 | 100 | 10 | 1 | 0.6085 | 0.5934 | 2.48 | 0.6085 | 0 | t |
| 30 | 100 | 10 | 2 | 0.4658 | 0.5238 | 12.44 | 0.4929 | 5.82 | c |
| 31 | 100 | 10 | 3 | 1.1964 | 1.1040 | 7.73 | 1.1964 | 0 | t |
| 32 | 100 | 12 | 1 | 0.6100 | 0.6433 | 5.46 | 0.6100 | 0 | t |
| 33 | 100 | 12 | 2 | 0.7939 | 0.6112 | 23.01 | 0.7939 | 0 | t |
| 34 | 100 | 12 | 3 | 1.0500 | 1.2240 | 16.57 | 1.0583 | 0.79 | c |
| | | | | | Average | 11.13 | | 3.53 | |
| | | | | | MSE | 14.15 | | 7.71 | |
| | | | | | $R^2$ | 0.8583 | | 0.9614 | |

*t* training data set for ANN learning, *c* testing data set for ANN learning

Meanwhile, two local concave surfaces where found on the response surface; on one of the local concave surfaces, the minimal form accuracy of the lens was 0.3030 μm, with a cooling time of 11.1 s and a packing time of 2.5544 s; on the other local concave surface, the minimal form accuracy of the lens was 0.3155 μm, with a cooling time of 12.2 s and a packing time of 1.4027 s. Table 9 shows the minimal form accuracy of the lens at three mold temperatures. In summary, for ANN model, the optimal form accuracy of the lens was 0.2398 μm, with a mold temperature of 85 °C, a cooling time of 10 s, and a packing time of 2.2403 s. Compared with the RSM model in which an optimal form accuracy of 0.3758 μm was obtained, the ANN model had a superior lens form accuracy.

As indicated in contour distributions for the two models, the parameter data near the center of the concave surface are

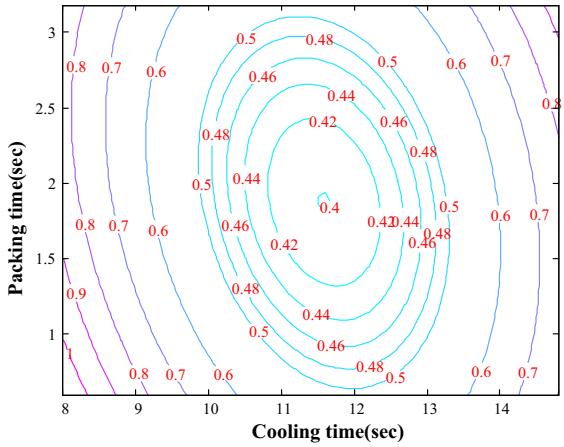


(a) RSM model at mold temperature of 70°C.

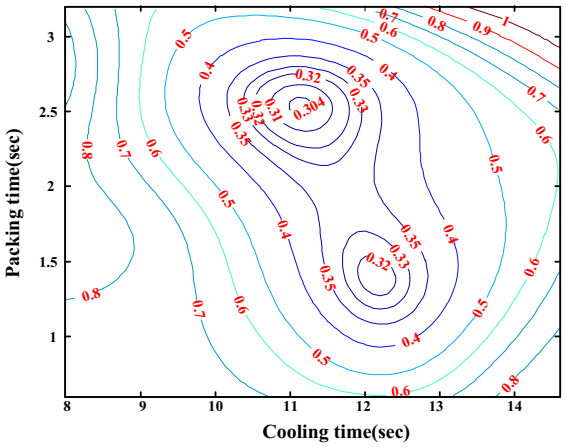


(b) ANN model at mold temperature of 70°C.

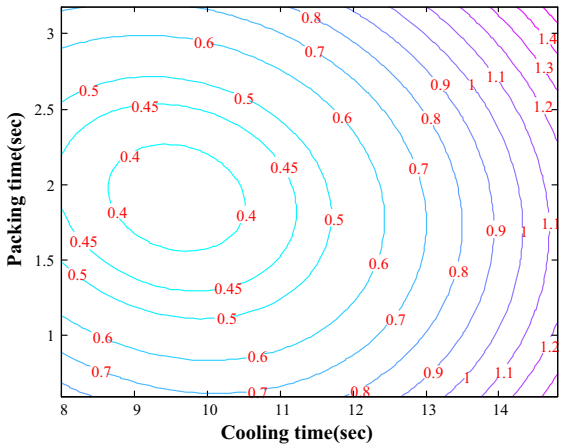


(c) RSM model at mold temperature of 85°C.

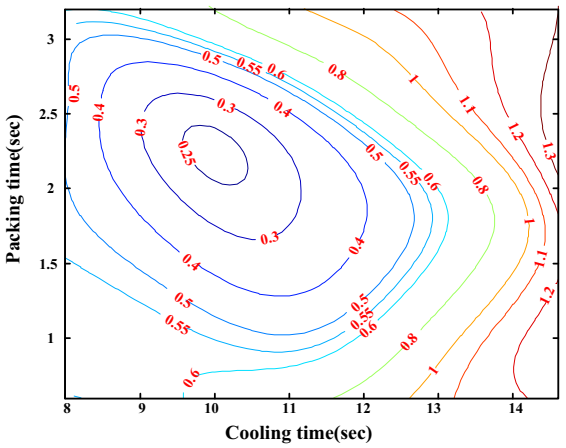


(d) ANN model at mold temperature of 85°C.

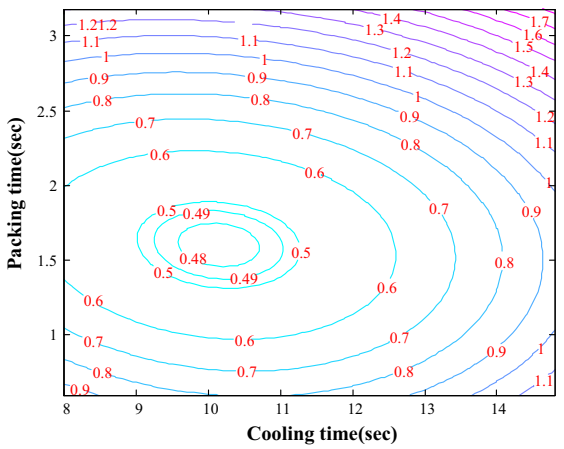


(e) RSM model at mold temperature of 100°C.

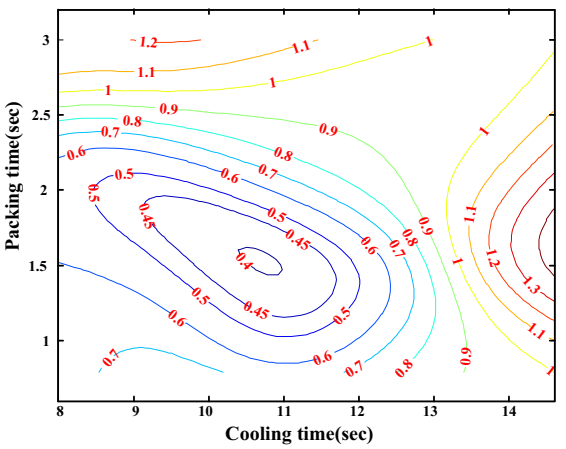


(f) ANN model at mold temperature of 100°C.

**Fig. 6** Contours for the form accuracy of the lens at various mold temperatures for the two models: RSM model at mold temperatures of 70 °C (**a**), 85 °C (**c**), and 100 °C (**e**); ANN model at mold temperatures of 70 °C (**b**), 85 °C (**d**), and 100 °C (**f**)

almost identical. The surface has a larger gradient along with packing time directing, which means that packing time is the more significant factor affecting form accuracy of the lens, compared to cooling time. Also, the effect of packing time on form accuracy of the lens increases with increasing mold temperature; however, the cooling time has a similar effect on form accuracy of the lens among the three mold temperatures.

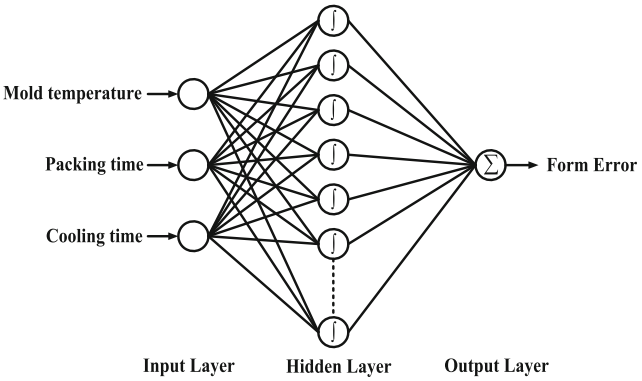


**Fig. 7** The architecture of ANN

### 4.3 Establish process window for injection molding

The response surface constructed by Eq. (5) using the form accuracy of the lens was a quadratic model of three injection molding parameters; the shape of the contour map drawn based on the equation was oval-like. This study therefore uses an elliptic equation to fit the point coordinates of the contour. The center of the fitted oval corresponds to the optimal form accuracy value and the process conditions required. First, the quality characteristic value is specified, and the mold temperature and cooling time to be fitted are then substituted in the RSM and ANN models to determine the packing time. The values of the cooling time and packing time are the point coordinates of the contour to be elliptically fitted. The elliptic parameter equations for fitting are

$$\begin{cases} x = \mathrm{Rx} \times \cos t \times \cos\theta - \mathrm{Ry} \times \sin t \times \sin\theta + \mathrm{Cx} \\ y = \mathrm{Rx} \times \cos t \times \sin\theta + \mathrm{Ry} \times \sin t \times \cos\theta + \mathrm{Cy} \end{cases} \quad (6)$$

where $x$ and $y$ are the parametric form of the elliptic equation, respectively; Rx and Ry are the half lengths of major axis and minor axis, respectively; $t$ is the parametric variable, and its value is $0 \leqq t \leqq 2\pi$; $\theta$ is the angle between the major axis and the horizontal line; and Cx and Cy are the $x$ and $y$ coordinates of the center point of the ellipse.

Point coordinates can be fitted in approximate ellipse by the least square method. This elliptical region is the process window for injection molding. Taking the form accuracy of 0.5 μm as an example, Fig. 8 shows the fit results of RSM and ANN models at different mold temperatures. The figure was constructed using the approximate coordinate scale, and the close contours are the process window of injection molding for the designated form accuracy of the lens. The figure revealed that, for both models, the effect of packing time on form accuracy of the lens was more significant compared with that of the cooling time. Therefore, in the process window for the form accuracy of 0.5 μm, the setting range of cooling time was larger than that of the packing time, irrespective of mold temperatures.

**Table 8** Comparison of the number of different hidden nodes

| Hidden nodes | Epochs | $R^2$ |
|---|---|---|
| 6 | 2000 | 0.7841 |
| 8 | 2000 | 0.8342 |
| 10 | 2000 | 0.8902 |
| 12 | 2000 | 0.7823 |
| 14 | 2000 | 0.7661 |

**Table 9** Optimal form accuracy with parameters for ANN model at various mold temperatures

| Mold temp (°C) | Cool time (s) | Pack time (s) | PV (μm) |
|---|---|---|---|
| 70 | 11.1 | 2.5544 | 0.3030 |
| 70 | 12.2 | 1.4027 | 0.3155 |
| 85 | 10.0 | 2.2403 | 0.2398 |
| 100 | 10.7 | 1.5375 | 0.3970 |

According to the results, the process window at different mold temperatures obtained by RSM is an oblique oval, and the experimental points are almost dispersed over the elliptical contour as shown in Fig. 8a, c, e. The angle between the major axis of oval and the horizontal axis decreases with increasing mold temperature. The process windows of ANN model at various mold temperatures present an irregular contour as shown in Fig. 8b, d, f. In summary, for contour lines of ANN model, the angle between the major axis of oval and the horizontal axis also decreases with increasing mold temperature.

Equation (6) was used to implement curve fittings and the results are shown in Table 10, where the coefficient of the elliptical process window and the fitting coefficient of determination are presented; for a given lens form accuracy, the injection molding process parameter values can be identified as the center of the oval. Since higher-order logarithmic sigmoid function was used to establish the ANN model, oblong-oval contours were observed near the center of response surface, unlike the elliptical contours derived from RSM model. Even if a second-order elliptic equation was used for curve fitting and the errors were larger, least square fit can still be used to determine an ellipse with which process conditions for near-optimal form accuracy can be identified and confirmation experiments can be performed accordingly. Comparing the two models at different mold temperatures, the major and minor axes determined by using ANN model were both larger than those by RSM model, that is, the ranges of both parameters in the process window identified by ANN were larger than those by RSM. The angle between the major axis of contour identified by ANN model and the horizontal axis was also larger than that by RSM model; this again suggested that

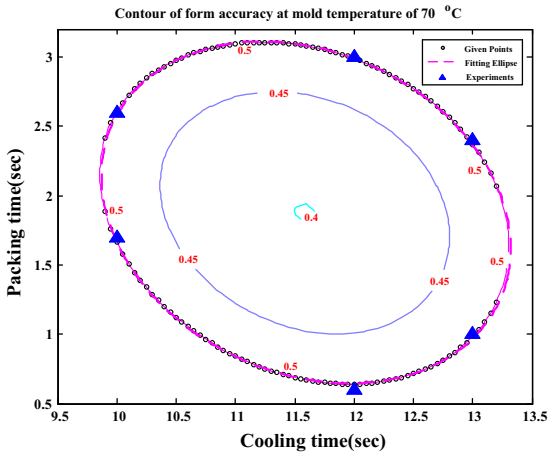


(a) RSM model at mold temperature of 70°C.

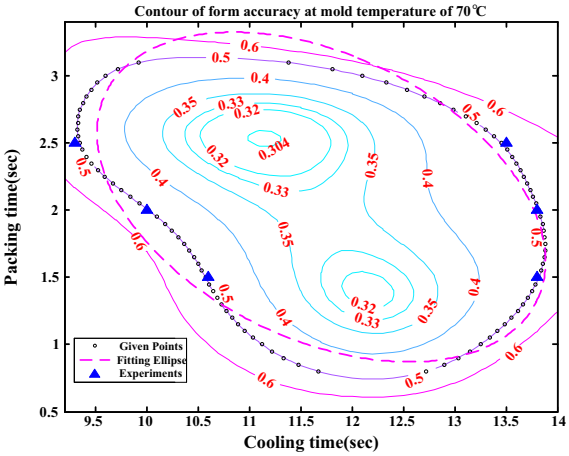


(b) ANN model at mold temperature of 70°C

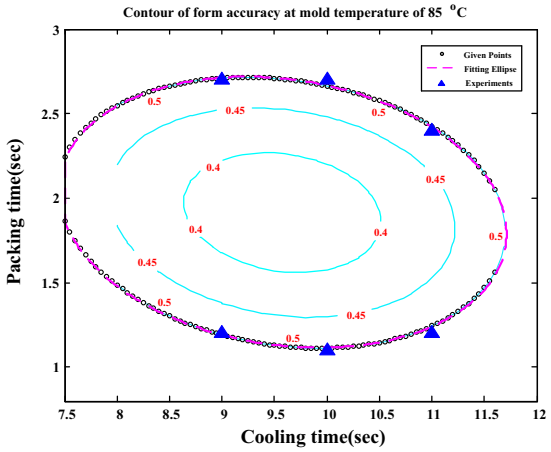


(c) RSM model at mold temperature of 85°C.

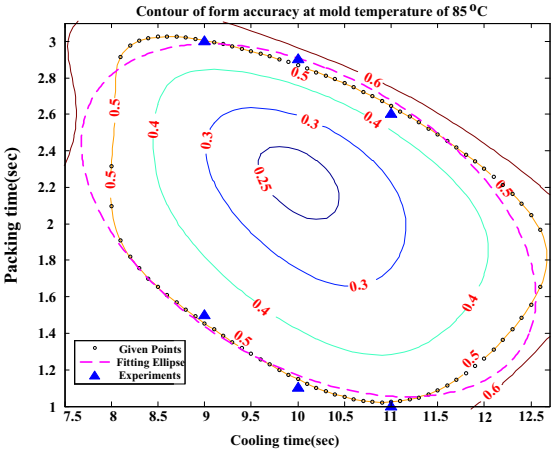


(d) ANN model at mold temperature of 85°C

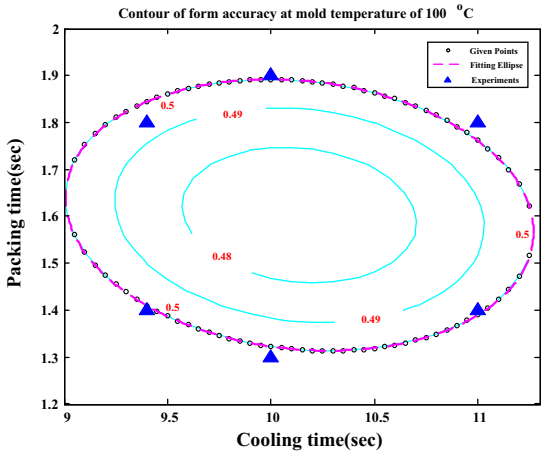


(e) RSM model at mold temperature of 100°C.

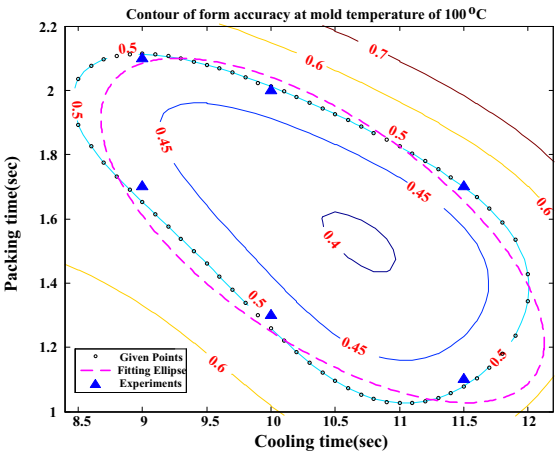


(f) ANN model at mold temperature of 100°C

**Fig. 8** Process windows for the lens with a form accuracy of 0.5 μm at various mold temperatures for the two models: RSM model at mold temperatures of 70 °C (**a**), 85 °C (**c**), and 100 °C (**e**); ANN model at mold temperatures of 70 °C (**b**), 85 °C (**d**), and 100 °C (**f**)

the ranges of parameters identified by ANN model were larger.

Moreover, comparing the process parameters for optimal form accuracy identified by the two models, the difference was only 0 to 0.5 s. At a mold temperature of 85 °C, the greatest difference in cooling time was 0.5 s, which means that the process parameters for optimal form accuracy identified by both models are almost identical.

**Table 10** Coefficients and $R^2$ of the fitted ellipse for process windows

| Mold temp (°C) | PV (μm) | Cx | Cy | Rx | Ry | Deg. | $R^2$ |
|---|---|---|---|---|---|---|---|
| Regression model with RSM | | | | | | | |
| 70 | 0.3997 | 11.5953 | 1.8786 | 1.7618 | 1.1791 | −15.8657 | 0.9917 |
| 85 | 0.3758 | 9.5785 | 1.9173 | 2.1376 | 0.7891 | −4.0252 | 0.9987 |
| 100 | 0.4733 | 10.1387 | 1.6033 | 1.1321 | 0.2868 | −1.9766 | 0.9998 |
| ANN model with RSM | | | | | | | |
| 70 | 0.3348 | 11.7066 | 2.1031 | 2.2384 | 1.1039 | 73.5267 | 0.9592 |
| 85 | 0.2510 | 10.1165 | 2.019 | 2.4773 | 0.8558 | 78.8337 | 0.9826 |
| 100 | 0.4004 | 10.4011 | 1.5637 | 1.7622 | 0.3987 | −12.0595 | 0.9642 |

Table 11 shows the confirmation experiment on the optimal form accuracy value of the lens. Although the difference in process parameter values for optimal form accuracy by the both models is very small, the ANN model has a better fitness; therefore, the predicted value of ANN model for optimal form accuracy was better than that of RSM model. According to the experimental results, the process window established by ANN model results in a better lens form accuracy than that of RSM model. When the mold temperature is 85 °C, cooling time is 9.6 s, and packing time is 1.9 s, the optimal lens form accuracy of RSM model is 0.3461 μm. The error to the predicted value is 8.58 %. When the mold temperature is 85 °C, cooling time is 10.1 s, and packing time is 2 s, the near-optimal lens form accuracy of ANN model is 0.2945 μm. The error is 13.98 % according to experimental verification. Although both the predicted and experimental values for optimal form accuracy were better by ANN model, the mean error was larger than that by RSM model. Considering the empirical apparatus used in this study was a hydraulic-driven injection molding machine, and accessing the resolution and stability of the machine, the error was within reasonable range.

### 4.4 Confirmation of process windows for two models

In order to verify the accuracy of the injection molding process window, six experimental conditions are selected at each mold temperature for the confirmation experiment. The error between the experimental value and the predicted value of the regression model is calculated as follows:

$$\text{Error}(\%) = \left|\frac{\text{Experimental results} - \text{Predictions}}{\text{Experimental results}}\right| \times 100\% \quad (7)$$

Taking a form accuracy of 0.5 μm as an example, two packing times were adopted for each of the three cooling times for RSM models and two cooling times were adopted for each of the three packing times for ANN models. The points for confirmation experiments were located on the form accuracy contour lines of the two models. The results of experiments are shown in Table 12 and Fig. 8. The results show that the maximum error between the experimental value and the predicted value for RSM model is 19.27 %, the smallest error is 2.31 %, and the average of error is 10.58 %. In addition, the maximum error for ANN model is 13.32 %, the smallest error is 0.95 %, and the average of error is 7.43 %. Therefore, the process window established by ANN has a smaller average error and better accuracy. The result confirmed what was mentioned above that the ranges of both parameters in the process window identified by ANN model were larger

**Table 11** Results of confirmation experiments for lens with optimal form accuracy at various mold temperatures

| Mold temp (°C) | Cool time (s) | Pack time (s) | Exp. PV (μm) | Pred. PV (μm) | Error (%) |
|---|---|---|---|---|---|
| Regression model with RSM | | | | | |
| 70 | 11.6 | 1.9 | 0.4332 | 0.3998 | 7.74 |
| 85 | 9.6 | 1.9 | 0.3461 | 0.3758 | 8.58 |
| 100 | 10.1 | 1.6 | 0.5114 | 0.4733 | 7.47 |
| | | | | Average | 7.92 |
| ANN model with RSM | | | | | |
| 70 | 11.7 | 2.1 | 0.3836 | 0.3348 | 12.73 |
| 85 | 10.1 | 2.0 | 0.2945 | 0.2533 | 13.98 |
| 100 | 10.4 | 1.6 | 0.4447 | 0.3999 | 10.08 |
| | | | | Average | 12.26 |

**Table 12** Results of confirmation experiments for process window of lens with a form accuracy of 0.5 μm

| Run | Mold temp (°C) | Cool time (s) | Pack time (s) | Exp. PV (μm) | Error (%) |
|---|---|---|---|---|---|
| Regression model with RSM | | | | | |
| 1 | 70 | 10 | 2.6 | 0.4727 | 5.78 |
| 2 | 70 | 10 | 1.7 | 0.4887 | 2.31 |
| 3 | 70 | 12 | 3 | 0.4832 | 3.49 |
| 4 | 70 | 12 | 0.6 | 0.4258 | 17.44 |
| 5 | 70 | 13 | 2.4 | 0.6066 | 17.57 |
| 6 | 70 | 13 | 1 | 0.6194 | 19.27 |
| 7 | 85 | 9 | 2.7 | 0.5255 | 4.85 |
| 8 | 85 | 9 | 1.2 | 0.5714 | 12.50 |
| 9 | 85 | 10 | 2.7 | 0.5392 | 7.27 |
| 10 | 85 | 10 | 1.1 | 0.5241 | 4.59 |
| 11 | 85 | 11 | 2.4 | 0.4827 | 3.59 |
| 12 | 85 | 11 | 1.2 | 0.5985 | 16.46 |
| 13 | 100 | 9.4 | 1.8 | 0.5572 | 10.26 |
| 14 | 100 | 9.4 | 1.4 | 0.5629 | 11.17 |
| 15 | 100 | 10 | 1.9 | 0.4782 | 4.57 |
| 16 | 100 | 10 | 1.3 | 0.5839 | 14.37 |
| 17 | 100 | 11 | 1.8 | 0.6072 | 17.65 |
| 18 | 100 | 11 | 1.4 | 0.6040 | 17.22 |
| | | | | Average | 10.58 |
| ANN model with RSM | | | | | |
| 1 | 70 | 10.6 | 1.5 | 0.5257 | 4.89 |
| 2 | 70 | 13.8 | 1.5 | 0.5721 | 12.61 |
| 3 | 70 | 10 | 2 | 0.5627 | 11.14 |
| 4 | 70 | 13.8 | 2 | 0.5351 | 6.55 |
| 5 | 70 | 9.3 | 2.5 | 0.4794 | 4.30 |
| 6 | 70 | 13.5 | 2.5 | 0.5418 | 7.72 |
| 7 | 85 | 9 | 1.5 | 0.4545 | 10.01 |
| 8 | 85 | 9 | 3 | 0.5282 | 5.34 |
| 9 | 85 | 10 | 1.1 | 0.5392 | 7.27 |
| 10 | 85 | 10 | 2.9 | 0.5263 | 4.99 |
| 11 | 85 | 11 | 1 | 0.4412 | 13.32 |
| 12 | 85 | 11 | 2.6 | 0.5048 | 0.95 |
| 13 | 100 | 9 | 1.7 | 0.5486 | 8.86 |
| 14 | 100 | 9 | 2.1 | 0.549 | 8.93 |
| 15 | 100 | 10 | 1.3 | 0.4782 | 4.57 |
| 16 | 100 | 10 | 2 | 0.5249 | 4.74 |
| 17 | 100 | 11.5 | 1.1 | 0.5664 | 11.72 |
| 18 | 100 | 11.5 | 1.7 | 0.5311 | 5.86 |
| | | | | Average | 7.43 |

than those by RSM model; therefore, the injection molding process window identified by ANN model was larger and the form accuracy produced was better, despite the irregular shape of process window.

## 5 Conclusion

This study used two methods to establish the spherical lens form accuracy prediction model and proposed the method to obtain the process window of injection molding parameters. The appropriate process parameters were obtained by designating the quality characteristics of molded products. The conclusions are proposed as follows:

1. The injection molding process window of cooling time and packing time is obtained by RSM and ANN. A quadratic polynomial function was used to establish the response surface of RSM model, and the contour near the center of the surface was an oblique oval. For ANN model, a higher-order logarithmic sigmoid function was used, and the contour near the center of the surface was a higher-order irregular curve. Comparing the two models, ANN model has a better fitness and accuracy.
2. An optimal form accuracy of 0.2398 μm was achieved at a mold temperature of 85 °C by ANN model, superior to the 0.3758 μm form accuracy by RSM model.
3. According to experimental verification, the predicted optimal form accuracy by RSM is 0.3758 μm and the error is 8.58 %, whereas the predicted near-optimal form accuracy by ANN is 0.2533 μm and the error is 13.98 %. The result also confirmed that the cooling time and packing time for the form accuracy identified by both models are almost identical.
4. The lens form accuracy of 0.5 μm is taken as an example for confirmation experimentation on the injection molding process window, and the process window established using ANN method has a better accuracy. The results confirmed that the ranges of both parameters, cooling time and packing time, in the process window identified by ANN model were larger than those by RSM model.

**Acknowledgments** The authors are obliged to thank the National Science Foundation, Taiwan, Republic of China, for the project fund (NSC100-2221-E-167-011).

## References

1. Kurt M, Kaynak Y, Kamber OS, Mutlu B, Bakir B, Koklu U (2010) Influence of molding conditions on the shrinkage and roundness of injection molded parts. Int J Adv Manuf Technol 46:571–578
2. Park K (2004) A study on flow simulation and deformation analysis for injection-molded plastic parts using three-dimensional solid element. Polym Plast Technol Eng 43:1569–1585
3. Li H, Guo Z, Li D (2007) Reducing the effects of weldlines on appearance of plastic products by Taguchi experimental method. Int J Adv Manuf Technol 32:927–931
4. Taguchi G, Chowdhury S, Wu Y (2005) Taguchi's quality engineering handbook. John Wiley Sons, Hoboken

5. Montgomery DC (2001) Design and analysis of experiments, 3rd edn. Wiley, New York
6. Peace GS (1993) Taguchi methods. Addison-Wesley, Taipei
7. Yang C, Hung SW (2004) Optimizing the thermoforming process of polymeric foams: an approach by using the Taguchi method and the utility concept. Int J Adv Manuf Technol 24:353–360
8. Shiou FJ, Chen CCA, Li WT (2006) Automated surface finishing of plastic injection mold steel with spherical grinding and ball burnishing processes. Int J Adv Manuf Technol 28:61–66
9. Mahapatra SS, Patnaik A (2007) Optimization of wire electrical discharge machining (WEDM) process parameters using Taguchi method. Int J Adv Manuf Technol 34:911–925
10. Tang SH, Tan YJ, Sapuan SM, Sulaiman S, Ismail N, Samin R (2007) The use of Taguchi method in the design of plastic injection mould for reducing warpage. J Mater Proc Technol 182:418–426
11. Tsai KM (2010) Effect of injection molding process parameters on optical properties of lenses. Appl Opt 49:6149–6159
12. Altan M (2010) Reducing shrinkage in injection moldings via the Taguchi, ANOVA and neural network methods. Mater Des 31:599–604
13. Chiang YC, Cheng HC, Huang CF, Lee JL, Lin Y, Shen YK (2011) Warpage phenomenon of thin-wall injection molding. Int J Adv Manuf Technol 55:517–526
14. Öktem H (2012) Optimum process conditions on shrinkage of an injected-molded part of DVD-ROM cover using Taguchi robust method. Int J Adv Manuf Technol 61:519–528
15. Modrak V, Mandulak J, Marton D (2013) Investigation of the influence of technological parameters on surface color of plastic parts. Int J Adv Manuf Technol 69:1757–1764
16. Sadeghi BHM (2000) A BP-neural network predictor model for plastic injection molding process. J Mater Proc Technol 103:411–416
17. Kwak TS, Suzuki T, Bae WB, Uehara Y, Ohmori H (2005) Application of neural network and computer simulation to improve surface profile of injection molding optic lens. J Mater Proc Technol 170:24–31
18. Lee KS, Lin JC (2006) Design of the runner and gating system parameters for a multi-cavity injection mould using FEM and neural network. Int J Adv Manuf Technol 27:1089–1096
19. Yen C, Lin JC, Li W, Huang MF (2006) An abductive neural network approach to the design of runner dimensions for the minimization of warpage in injection mouldings. J Mater Proc Technol 174:22–28
20. Shie JR (2008) Optimization of injection molding process for contour distortions of polypropylene composite components by a radial basis neural network. Int J Adv Manuf Technol 36:1091–1103
21. Chen WC, Wang MW, Chen CT, Fu GL (2009) An integrated parameter optimization system for MISO plastic injection molding. Int J Adv Manuf Technol 44:501–511
22. Chen CC, Su PL, Lin YC (2009) Analysis and modeling of effective parameters for dimension shrinkage variation of injection molded part with thin shell feature using response surface methodology. Int J Adv Manuf Technol 45:1087–1095
23. Yin F, Mao H, Hua L (2011) A hybrid of back propagation neural network and genetic algorithm for optimization of injection molding process parameters. Mater Des 32:3457–3464
24. Huang CN, Chang CC (2011) Optimal-parameter determination by inverse model based on MANFIS: the case of injection molding for PBGA. IEEE Trans Control Syst Technol 19:1596–1603
25. Tzeng CJ, Yang YK, Lin YH, Tsai CH (2012) A study of optimization of injection molding process parameters for SGF and PTFE reinforced PC composites using neural network and response surface methodology. Int J Adv Manuf Technol 63:691–704
26. Myers RH, Montgomery DC (2002) Response surface methodology: process and product optimization using designed experiments, 2nd edn. Wiley, New York
27. Bas D, Boyaci IH (2007) Modeling and optimization I: usability of response surface methodology. J Food Eng 78:836–845
28. Lizotte DJ, Greiner R, Schuurmans D (2012) An experimental methodology for response surface optimization methods. J Glob Optim 53:699–736
29. Chiang KT, Chang FP (2007) Analysis of shrinkage and warpage in an injection-molded part with a thin shell feature using the response surface methodology. Int J Adv Manuf Technol 35:468–479
30. Wang G, Zhao G, Li H, Guan Y (2011) Research on optimization design of the heating/cooling channels for rapid heat cycle molding based on response surface methodology and constrained particle swarm optimization. Expert Syst Appl 38:6705–6719
31. Wua L, Yick KL, Ng SP, Yip J, Kong KH (2012) Parametric design and process parameter optimization for bra cup molding via response surface methodology. Expert Syst Appl 39:162–171
32. Kurtaran H, Erzurumlu T (2006) Efficient warpage optimization of thin shell plastics parts using response surface methodology and genetic algorithm. Int J Adv Manuf Technol 27:468–472
33. Brient A, Brissot M, Rouxel T, Sangleboeuf JC (2011) Influence of grinding parameters on glass workpieces surface finish using response surface methodology. J Manuf Sci Eng 133, doi:10.1115/1.4004317
34. Pradhan MK (2013) Estimating the effect of process parameters on surface integrity of EDMed AISI D2 tool steel by response surface methodology coupled with grey relational analysis. J Adv Manuf Technol 67:2051–2062
35. Tsai KM, Tang BH (2014) Determination of injection molding process window based on form accuracy of lens using response surface methodology. J Adv Manuf Technol 75:947–958